NMDA Receptors Control Cue-Outcome Selectivity and Plasticity of Orbitofrontal Firing Patterns during Associative Stimulus-Reward Learning

Marijn van Wingerden,[1,3,6] Martin Vinck,[1,6] Vincent Tijms,[2] Irene R.S. Ferreira,[4] Allert J. Jonker,[5] and Cyriel M.A. Pennartz[1,2,*]
[1]Swammerdam Institute for Life Sciences, Center for Neuroscience, Faculty of Science
[2]Research Priority Program Brain and Cognition
University of Amsterdam, Postal Box 94216, 1090 GE Amsterdam, the Netherlands
[3]Institute of Experimental Psychology, Heinrich-Heine University Düsseldorf, Universitaetsstrasse 1, D-40225 Düsseldorf, Germany
[4]Max Planck Institute of Neurobiology, 82152 Munich, Germany
[5]Department of Anatomy & Neurosciences, Free University Medical Center, v/d Boechorststraat 7; 1081 BT Amsterdam, Netherlands
[6]These authors contributed equally to this work
*Correspondence: c.m.a.pennartz@uva.nl
http://dx.doi.org/10.1016/j.neuron.2012.09.039

SUMMARY

Neural activity in orbitofrontal cortex has been linked to flexible representations of stimulus-outcome associations. Such value representations are known to emerge with learning, but the neural mechanisms supporting this phenomenon are not well understood. Here, we provide evidence for a causal role for NMDA receptors (NMDARs) in mediating spike pattern discriminability, neural plasticity, and rhythmic synchronization in relation to evaluative stimulus processing and decision making. Using tetrodes, single-unit spike trains and local field potentials were recorded during local, unilateral perfusion of an NMDAR blocker in rat OFC. In the absence of behavioral effects, NMDAR blockade severely hampered outcome-selective spike pattern formation to olfactory cues, relative to control perfusions. Moreover, NMDAR blockade shifted local rhythmic synchronization to higher frequencies and degraded its linkage to stimulus-outcome selective coding. These results demonstrate the importance of NMDARs for cue-outcome associative coding in OFC during learning and illustrate how NMDAR blockade disrupts network dynamics.

INTRODUCTION

An essential component of decision-making is the retrieval of values associated with stimuli and utilization of this information to select responses. Value is the net payoff, or outcome, that is predicted to occur in the future given a stimulus or state. Recent studies have shed light on the neuronal correlates of value representations in the brain and how stimulus-outcome associations are updated when task contingencies are changed (e.g., Padoa-Schioppa and Assad, 2006; Platt and Glimcher, 1999; Sugrue et al., 2005). Across several species, the OFC has been consistently implicated in coding and utilizing such representations during decision making. Stimuli elicit responses in orbitofrontal neurons that are sensitive to future outcome (Hikosaka and Watanabe, 2000; Padoa-Schioppa and Assad, 2006; Schoenbaum et al., 2009; Tremblay and Schultz, 2000a, 2000b; van Duuren et al., 2008; Wallis and Miller, 2003). Complementary lesion studies suggested a causal role of OFC in the updating of stimulus values and the assignment of credit to behavioral choices associated with positive or negative outcome (Baxter et al., 2000; Bohn et al., 2003b; Rolls et al., 1994; Schoenbaum et al., 2002, 2009; Walton et al., 2010). However, the neural mechanisms mediating these OFC functions are largely unknown. Because electrophysiological studies provide correlative data, it has also remained unknown whether neural representations of value depend on mechanisms within orbitofrontal cortex itself.

A promising starting point to investigate these mechanisms is the N-methyl-D-aspartate receptor (NMDAR). This is motivated by the glutamatergic nature of fast excitatory connections in OFC, including its thalamic and cortical afferents as well as intrinsic connections between its pyramidal cells (Hoover and Vertes, 2011; Seamans et al., 2003; Wang, 1999). NMDARs play a key role in synaptic plasticity, including both long-term potentiation and depression (Lee et al., 1998; Malenka and Nicoll, 1999; Selig et al., 1995). The role of NMDARs in mediating learning-related changes in neural excitability in vivo has been primarily studied in amygdala in relation to fear conditioning (Goosens and Maren, 2004; Li et al., 1995) and in hippocampus in relation to spatial memory (Ekstrom et al., 2001; Kentros et al., 1998; McHugh et al., 2007; Morris et al., 1986), but not in the context of associative stimulus-reward learning as exemplified by OFC neurons.

Schoenbaum et al. (1998, 1999) showed that, during learning, OFC neurons come to fire differentially to stimuli associated with distinct outcomes, but it is unknown whether this selectivity arises from local OFC mechanisms and depends on NMDAR

Cell
PRESS
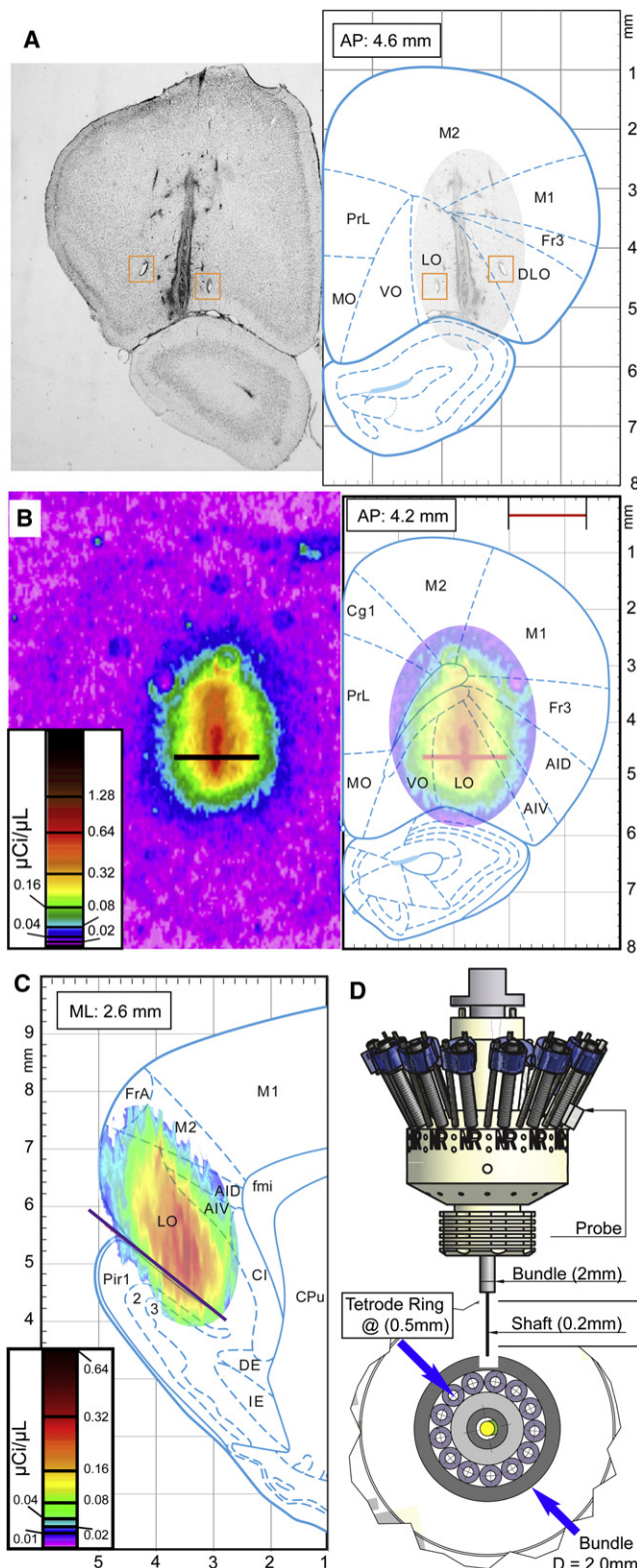
Figure 1. Histology and Autoradiography

(A) Grayscale photomicrograph of a Cresyl-Violet stained coronal section through OFC, showing the probe track and two tetrode endpoints. The cor-

activity. Apart from a hypothesized role in long-term plasticity of OFC firing patterns, NMDARs may contribute acutely to OFC information processing: under depolarized membrane voltages they contribute slow EPSP components to synaptic responses (Herron et al., 1986), and these may help solve, e.g., pattern discrimination and working-memory problems (Durstewitz et al., 2000; McHugh et al., 2007; Wang, 1999). By the same token, NMDARs may contribute to spike timing relative to the phase of oscillatory local field potentials (LFPs), as hypothesized for hippocampus (Buzsáki, 2002; Jensen and Lisman, 1996). If NMDARs modulate the strength of spike-LFP phase locking, they would be in a key position to affect the efficacy by which OFC output excites target areas (such as striatum and basolateral amygdala; Pennartz et al., 2011b) and to regulate downstream synaptic modifications by spike-timing-dependent plasticity (Bi and Poo, 1998; Cassenaer and Laurent, 2007).

We applied the technique of reverse microdialysis in combination with multitetrode recordings to study how NMDAR blockade affects discriminatory firing patterns and rhythmic mass activity in the OFC of rats learning stimulus-reward associations and reversals in an odor discrimination task (Schoenbaum et al., 1998; van Duuren et al., 2007a). We show that NMDARs affect discriminatory coding of OFC neurons especially during stimulus presentation and decision making and shape plasticity of discriminatory firing across learning trials. NMDAR blockade leads to hypersynchronous phase locking in the theta, beta, and high-frequency bands and destroys the functional relationship between theta-band phase-locking and discriminative power by virtue of firing rate. Unilateral blockade of NMDA receptors does not affect behavioral performance during task acquisition but hampers changes in reaction time after reversal of task contingencies.

RESULTS

We recorded 623 isolated single units from four rats in 20 counterbalanced sessions (number of sessions for drug/control = 10/10) using a modified microdrive that held 12 tetrodes arranged concentrically around a microdialysis probe (Figure 1). Histological verification indicated that most recordings were from ventral and lateral orbitofrontal (VO/LO) and agranular insular (AI) cortex with some spread into dorsolateral orbitofrontal (DLO) cortex (Figure 1A). For each rat, recordings were obtained under both drug and control conditions. However, within a single session, only one condition was applied. In drug sessions, we used continuous reverse microdialysis to apply a 0.5 mM solution of

responding plate from the rat brain atlas by Paxinos and Watson (2007) is shown for comparison.

(B) Calibrated autoradioactivity levels as a function of stereotaxic space in a coronal section. Spread of activity from the probe is ellipsoid rather than spherical, because diffusion took place along a membrane spanning 2 mm DV. Black bar indicates diameter of the tetrode ring (approx. 1.4 mm).

(C) Sagittal reconstruction of anterior-posterior spread of radioactivity, based on averaged coronal activity (see Supplemental Experimental Procedures). Purple line indicates alignment of sequential coronal activity profiles to the estimated orbitofrontal-piriform cortex border.

(D) Side and bottom view (not to scale) of the combidrive, holding a concentric ring of tetrodes around a microdialysis probe.
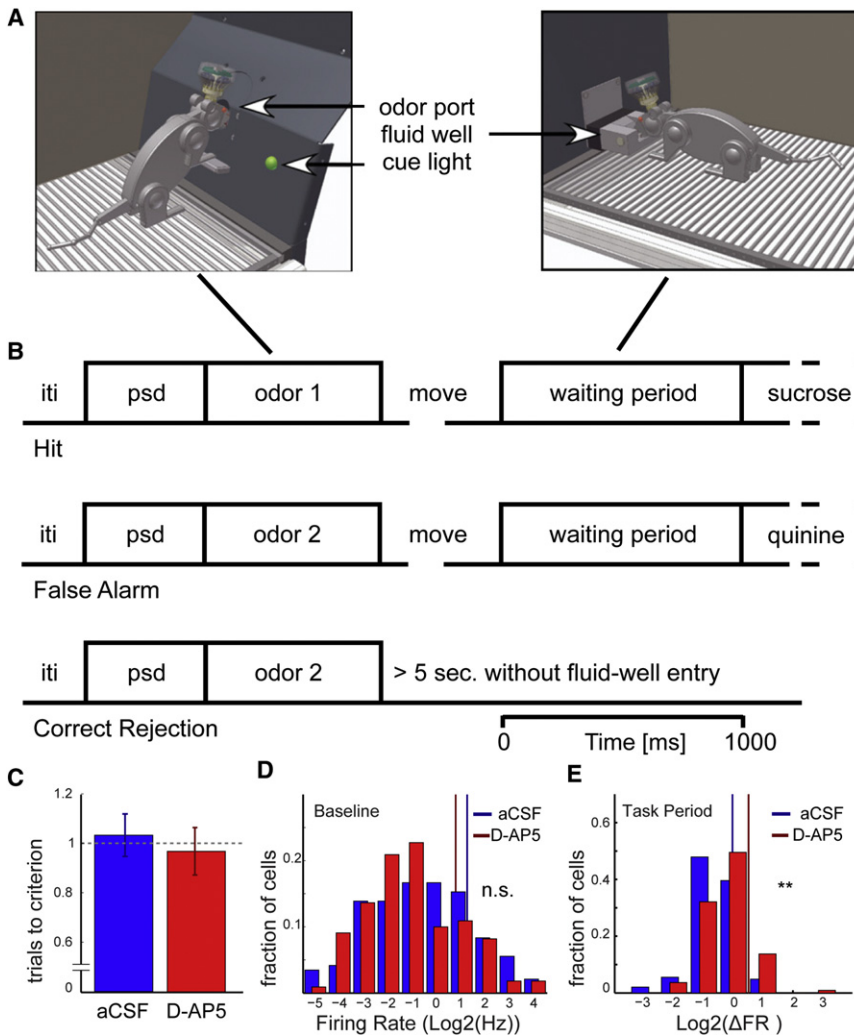
Figure 2. Behavioral Task and Effect of D-AP5 on Raw and Relative Firing Rates

(A) Operant chamber; impression of rat making odor poke (left) and fluid poke (right).

(B) Trial types; sequence of task elements on hit, false alarm, and correct rejection trials. Iti, intertrial interval; psd, prestimulus delay.

(C) Average number (±SEM) of trials to criterion, normalized per rat to the average number of trials to criterion for drug and control sessions for that rat.

(D) Histogram of $\log_2$ transformed baseline firing rates. Vertical lines correspond to mean firing rates.

(E) Histogram of $\log_2$ transformed relative firing rates to baseline during engagement in the task (averaged from odor onset to outcome delivery). A value of zero indicates that task and baseline firing rate were equal. Conventions as in (D). **$p < 0.01$ (Mann-Whitney U test).

(A) and (B) adapted from (van Wingerden et al., 2010a). See also Figure S1.

D-2-amino-5-phosphonopentanoate (D-AP5), a competitive NMDAR blocker, dissolved in aCSF. A separate autoradiography experiment with ^{3}H-D-AP5 confirmed that the concentration of D-AP5 in OFC was sufficient to antagonize NMDARs (Figures 1B and 1C). Infusions were done unilaterally to minimize the chance of inducing behavioral effects, which could confound the interpretation of electrophysiological results if present.

NMDA Receptor Blockade and Behavioral Performance

Rats performed a two-odor, go/no-go discrimination task, with novel odor-outcome associations for each session (Figures 2A and 2B; Schoenbaum et al., 1998; van Duuren et al., 2007a; van Wingerden et al., 2010a, 2010b). Task acquisition was manifested by the emergence of "No-go" and "Go" responses to the odors predicting a negative (S− condition; "correct rejections") and positive outcome (S+ condition; "hits"), respectively. The acquisition phase of the task was terminated when rats reached a behavioral criterion (85% correct trials, i.e., hits + correct rejections, in a moving 20-trial block), after which a reversal phase followed, in which the previously presented stimulus-outcome pairings were switched. We first examined overall

task performance, defined as the average number of trials to reach criterion, normalized per rat to the average number of trials to criterion for all drug and control sessions for that rat. Overall performance did not differ between control and drug sessions (mean ± SEM; control: 103% ± 8.6%, drug: 96.7% ± 9.6%, two-sided t test n.s.; Figure 2C). Reaction time (RT), i.e., the time between odor poke termination and subsequent fluid well entry, decreased with acquisition trial number in the S+ condition for both the control (Spearman's rho = −0.24, p < 0.01) and drug condition (rho = −0.17, p < 0.05; difference in slopes between conditions n.s., Fisher's Z test: p = 0.31), but not in the S− condition ("false alarm trials"; p values: 0.82 [aCSF] and 0.24 [D-AP5]). RT was faster for hits than false alarm trials, both for control and drug sessions (p < 0.001 and p < 0.05, respectively; Mann-Whitney U test). No significant difference in RT between control and drug sessions was detected, neither for hits nor false alarms (p = 0.07 and p = 0.23, respectively; Mann-Whitney U test). Altogether, the absence of significant behavioral differences between the drug and control condition for the task acquisition phase, indicates that electrophysiological comparisons between these two conditions can be made in a comparable behavioral context.

This finding contrasts with the early reversal phase, where we did observe an effect of unilateral D-AP5 infusion. Here, the mean Z-scored RT after reversal differed significantly from the last 10 trials before reversal for both S+ to S− and S− to S+ transitions in control (p < 0.01, Mann-Whitney U test; see Figure S1 available online), but not drug sessions (p = 0.28, p = 0.76, respectively). Direct comparisons between RTs indicated that RT for aCSF and D-AP5 sessions did not differ for the last 10

Table 1. Firing Rate Comparisons between aCSF and D-AP5 Units

	Baseline (Hz)	Odor (Hz)		Move (Hz)		Wait (Hz)	
Raw FR aCSF; 144 cells	2.35 ± 0.33	2.37 ± 0.38		2.56 ± 0.40		2.37 ± 0.39	
Raw FR D-AP5; 110 cells	1.78 ± 0.32	2.36 ± 0.43		2.01 ± 0.28		1.96 ± 0.32	
FR (% of base) aCSF	—	94 ± 4.7%	†	104 ± 7.3%	†	103 ± 6.4%	†
FR (% of base) D-AP5	—	136 ± 13%**		142 ± 21%		138 ± 10% ***	

Table 1 depicts the raw firing rate (FR) of putative pyramidal cells recorded under aCSF (n = 144 of 164 aCSF cells) or D-AP5 (n = 110 of 117 D-AP5 cells) conditions, as well as firing rates relative to baseline (set at 100%). Baseline was defined as −3 to −1 s before odor onset, the odor period (Odor) as 0 to +1 s after odor onset, the movement period (Move) as 0 to +1 s after odor offset, and the waiting period (Wait) as −1 to 0 s before outcome delivery. Group averages ± SEM are reported.
†Significant differences between group (aCSF, D-AP5) means, p < 0.01 Mann-Whitney U-test.
,*group mean significantly greater than baseline (100%), p < 0.01, 0.001, one-sample t test versus 1).

trials before reversal (p > 0.05 for both S+ and S− trials, Mann-Whitney U test). Postreversal, however, we found significant differences in Z-scored RT between pharmacological conditions for both S+ (ACQ) trials, now S− and S− (ACQ) trials, now S+ (p < 0.001 and p < 0.05, respectively, Mann-Whitney U test).

Effect of NMDA Receptor Blockade on Firing Rates

Out of the 623 recorded cells, 281 (117 for D-AP5, 164 for aCSF) units were included for further analysis because of their responsiveness to perfusion (see Experimental Procedures). Unless stated otherwise, all further analyses pertain to the acquisition phase of the task. After exclusion of putative fast-spiking interneurons (N_{aCSF} = 20; N_{D-AP5} = 7) based on waveform characteristics (van Wingerden et al., 2010b), we did not detect a significant difference in the mean raw firing rate of putative pyramidal cells between the control and drug condition for the ITI (intertrial interval) baseline period (FR_{aCSF} mean ± SEM: 2.35 ± 0.33 Hz, FR_{D-AP5}: 1.78 ± 0.32 Hz, n.s., Mann-Whitney U test; Figure 2D), and the three task periods leading up to the outcome (odor sampling, locomotion from odor port to fluid well, waiting period; Table 1). However, for all of these three task periods we found increased firing rates relative to baseline for the drug (across periods: mean ± SEM = 138% ± 9.5%, p < 0.01, Mann-Whitney U test; Figure 2E), but not for the control condition (102% ± 3.7%).

### Effect of NMDA Receptor Blockade on Discriminative Power of Firing Rates

To examine whether D-AP5 affected the firing rate discrimination between the S+ and S− condition, we performed an ROC (receiver operator characteristic) analysis (cf. Green and Swets, 1966; Histed et al., 2009). For each unit, we examined to what extent firing rates in fragments of 200 ms discriminated between S+ and S− by computing the shuffle-corrected ROC area, called $D_{corrected}$ (Figure 3): an index ranging from 0 (no discriminative power) to 1/2 (maximum discriminative power; negative numbers incidentally occur because of limited sampling). We then averaged $D_{corrected}$ across units, while balancing, for a given rat, the number of cells entered in the analysis across pharmacological conditions. In the acquisition phase, D-AP5 caused a decrease in $D_{corrected}$ values for the odor period (Figure 3; p < 0.01, Bootstrap test with Bonferroni correction). In this phase, no significant drug effects were found in phases following odor sampling.

In the reversal phase, D-AP5 significantly reduced $D_{corrected}$ values during the odor as well as early and late movement phases (Figure S2). Units' $D_{corrected}$ scores in the reversal phase may reflect the sign (direction) of their acquisition-phase firing rate selectivity or a reversed selectivity. In fact, maintenance of cue selectivity across cue-outcome reversal has been linked to faster reversal learning (Schoenbaum et al., 2007; Stalnaker et al., 2006). To assess the consistency of firing rate selectivity, we applied a sign function to the $D_{corrected}$ calculation. We found that, after reversal, firing rate selectivity was preserved especially in the odor sampling phase of control, but not drug sessions, whereas firing rate selectivities showed a mixture of maintenance and flips for the movement and waiting phases (Figures S3 and S4).

The observed effects of D-AP5 are unlikely to be a consequence of changes in the prevalence of firing-rate correlates. A unit was defined as having a firing-rate correlate for a given task period if its firing rate in that period differed significantly from the ITI firing rate. The distribution of firing rate correlates did not significantly differ between control and drug conditions across task periods (Table 2; chi-square test; df = 4; p = 0.64).

Plasticity in Discriminative Power of Firing Rates

One route by which D-AP5 may impact discriminatory firing is through the impairment of NMDAR-dependent, long-term synaptic plasticity, which may be required for neurons to develop stimulus-outcome discrimination across learning trials. Alternatively, NMDARs may acutely support discriminatory firing because of their slow EPSP contributions. If the effects of D-AP5 are mediated via long-term plasticity, they should gradually become more pronounced across trials. To investigate how effects of D-AP5 on outcome-selective firing patterns develop across trials, we examined single-trial contributions to ROC discrimination scores using a leave-one-out procedure, yielding pseudo discrimination (PD) scores per trial (see Experimental Procedures). A positive or negative PD score for a given trial indicated that inclusion of the trial had a positive or negative effect, respectively, on the overall ROC. PD scores were averaged across cells, separately for the odor, movement and waiting period. For both the S+ and S− trials in the odor period, we found an upward trend in average PD score over trials for the control condition, with higher PD values compared to the drug condition on later trials (p < 0.05, Bootstrap test against shuffled data; Figures 4A and 4B). To quantify the magnitude of changes in PD scores across trials, we first computed the mean difference
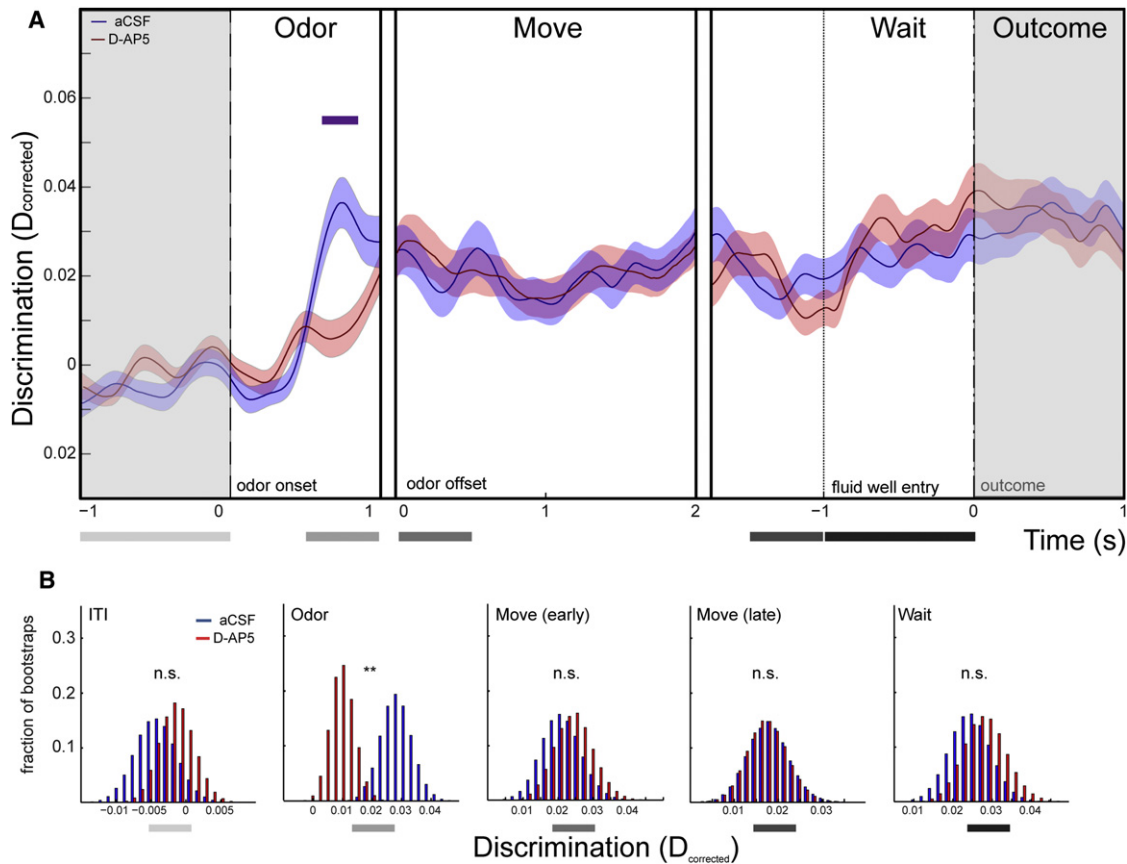
Figure 3. Discrimination of Firing Rates between S+ and S− Condition

(A) Bootstrapped mean of time-resolved $D_{corrected}$ values (shuffle-corrected ROC area), a measure of discrimination between S+ and S− trials. Time-resolved traces are presented in three abutting windows (thick black boxes): aligned to odor onset, aligned to odor offset, and aligned to outcome delivery. Shaded area corresponds to SD of bootstrapped population. Vertical dashed line: odor onset; vertical dotted line: fluid well entry; vertical dash-dotted line: outcome delivery. Horizontal purple line indicates significant difference at $p < 0.01$ (bootstrap test, Bonferroni corrected).

(B) Histograms of bootstrapped mean $D_{corrected}$ values for units recorded under aCSF and D-AP5 during acquisition at time windows indicated by grayscale horizontal bars on the time axis in (A). **significant difference in bootstrapped means, $p < 0.01$ (bootstrap test).

See also Figures S2–S4.

in average PD scores between the first and last trial. For both S+ and S− trials, this difference was higher than zero for the control, but not drug condition (Bootstrap test; $p < 0.05$, Figures 4E and 4F). The mean difference score was higher for control than drug units, for both trial types ($p < 0.01$, Bootstrap test).

Second, to model the relationship between mean PD score and trial number, we performed a regression analysis with a linear and exponential term. Best fits were obtained by iterative fitting (Figures 4C and 4D). For both the S+ and S− condition, linear and exponential parameters were significantly different from zero for the control (i.e., the 95% confidence interval for the fitted parameters did not contain zero), but not for the drug condition. Finally, we note that during the movement and waiting periods of control and drug sessions, the population averages of PD scores did not show a clear upward trend across trials, indicating an absence of significant plasticity of discrimination between trial types in these periods. Thus, with learning, the discriminability of spike train responses to odor stimuli slowly increased, and selectively so for the odor period. This process depends, at least

in part, on NMDAR function. Overall, we found no significant effect of D-AP5 on early learning trials, as would otherwise have supported a function of NMDARs on acute processing by slow EPSP contributions.

Effect of NMDA Receptor Blockade on Rhythmic Synchronization

In addition to affecting firing rates and discriminative coding, NMDARs may well regulate rhythmic mass activity as visible in LFPs, and concomitant entrainment of OFC neurons to these signals. We focused on odor sampling because of the strong changes in ROC discrimination scores during this period, and our previous finding of strong gamma- and theta-band synchronization during stimulus processing (van Wingerden et al., 2010b). In LFP signals, we found that D-AP5 induced a broad-band increase in relative power for the theta-band as well as frequencies above ~20 Hz and a concurrent decrease in low-frequency power ($p < 0.05$, Figure 5; multiple comparison corrected [MCC] permutation test on T statistics; Bullmore

Table 2. Distribution of Firing-Rate Correlates across Task Periods

Analyzed cells n = 281	Odor	Move	Wait	Outcome	NONE
aCSF sessions (n = 10) n = 164 cells	29 (17,6%)	22 (13,4%)	21 (12,8%)	27 (16,5%)	99 (60,3%)
D-AP5 session (n = 10) n = 117 cells	26 [21]	18 [16]	16 [15]	18 [19]	64 [71]

Distribution of cells recorded with a firing-rate change correlated to different task periods. Out of 281 analyzed cells, subsets responded to one or more of the following periods (such that the sum of percentages exceeds 100%). Odor: odor sampling period; Move: movement/locomotor period; Wait: waiting period; Outcome: fluid delivery period. Units in the NONE category did not exhibit significant firing-rate correlates. Percentages in parentheses denote the fraction of cells out of the total number recorded under aCSF. Numbers in brackets indicate the (rounded) expected numbers of cells with correlates in D-AP5 sessions given the relative frequency of these correlates in aCSF sessions. The distribution of cell counts over the five categories did not significantly differ between aCSF and D-AP5 sessions (chi-square test, df = 4, p = 0.64).

et al., 1999; Maris et al., 2007). We confirmed our previous finding that LFP gamma-band power increases with trial number and is predictive of learning (van Wingerden et al., 2010b). A similar increase in LFP gamma power with trial number was observed for the drug condition (Figure S5). However, we found theta power to be negatively correlated with trial number in the drug, but not control condition (significant difference in slopes between D-AP5 en aCSF; p < 0.05; MCC permutation test; Figure S5).

To investigate whether D-AP5 affects local phase-synchronization of single units, we computed the spike-LFP pairwise phase consistency (PPC; Vinck et al., 2010, 2012). D-AP5 had a three-fold effect (Figures 5C and 5D; p < 0.05, MCC permutation test on T statistics). First, it strongly increased theta locking (~10 Hz) by about 100%. Second, a beta (20–25 Hz) rhythm emerged, which was absent in the control condition. Third, it increased spike-LFP phase-locking in the supra-gamma range (110–160 Hz).

Finally, we tested whether D-AP5 altered the relationship between neuronal discrimination scores and spike-LFP phase-locking patterns. For the 0.5–1.0 s. period of odor sampling (during which ROC values peaked) we correlated the unit's time-resolved $D_{corrected}$ ROC values with their spike-LFP PPC values, separately for D-AP5 and aCSF. Differences in Spearman-rank correlations between the drug and control condition were observed in the theta and supra-gamma range (Figure 6A; p < 0.05; MCC permutation test). For the control condition, we found that spike-LFP theta PPC positively predicted $D_{corrected}$, with significant correlations peaking (Figure 6B; p < 0.05, MCC permutation test on difference in Spearman rhos) around the time when the $D_{corrected}$ values peaked (0.5–1 s after odor onset; Figure 3). However, in the same time window D-AP5 induced a negative correlation between $D_{corrected}$ and supra-gamma PPC values (Figures 6A and 6C).

DISCUSSION

In conditions where a unilateral NMDAR blockade in rat OFC did not affect task acquisition behavior and modestly increased task-related firing rates relative to baseline, we showed that this receptor plays a significant role in neural representations discriminating between stimulus-outcome conditions and plastic changes in firing patterns associated with learning these representations. Especially during odor processing and decision-making the capacity of OFC neurons to discriminate between cues predictive of different outcomes was impaired

by NMDAR blockade. In addition, NMDAR blockade increased local rhythmic synchronization, as indexed by spike-LFP phase-locking, particularly in the theta (~10 Hz), beta (20–30 Hz), and high-frequency range (110–150 Hz). Finally, we found a positive relationship between theta phase-locking and neuronal discrimination scores under control conditions, which was abolished by NMDAR blockade.

One concern, when examining drug effects on neurophysiological correlates of cognitive processes, is that the drug may affect behavior, which could in turn affect firing patterns in OFC known to represent relevant behavioral task components (Pennartz et al., 2011a; Schoenbaum et al., 2009). Bilateral infusion of NMDAR antagonist in OFC has been shown to increase impulsive responding and impair reversal learning (Bohn et al., 2003b). Therefore, we chose unilateral drug application, and indeed found that performance scores and reaction time (RT) during task acquisition did not significantly differ between pharmacological conditions (in line with, e.g., De Bruin et al., 2000). However, upon transition to the reversal phase, RT for hit and false alarm trials showed a characteristic flip in behavioral responding according to the reversed task rule in control sessions, while such a flip was absent in drug sessions (Figure S1). Changes in RT in this type of task are thought to depend on OFC function (Bohn et al., 2003a; Schoenbaum et al., 2003a), particularly during the reversal phase in which NMDARs have been implicated by a previous study (Bohn et al., 2003b). Here, we show that unilateral blockade of NMDARs produces a comparable deficit in shaping discriminatory behavior according to updated task rules.

Firing-Rate Effects of NMDA Receptor Blockade in Comparison to Previous Studies

Previous work indicated that systemic injections of a nonspecific, open-channel NMDAR blocker (MK-801) in freely moving rats leads to increments and decrements in average basal firing rates in putative pyramidal cells and fast spiking interneurons, respectively (Homayoun and Moghaddam, 2007, 2008; Jackson et al., 2004). Here, we perfused a competitive NMDAR antagonist (D-AP5) directly into the OFC and found that putative pyramidal cell firing rates during the ITI did not significantly differ between drug and control sessions (Figure 2D). However, drug infusion induced a significant increase in relative firing rate during the various task stages (Figure 2E). Thus, the results from the current and previous studies differ insofar as we did not observe an overall firing-rate elevation during the ITI, as was the case in (Homayoun and Moghaddam, 2007, 2008; Jackson et al., 2004).
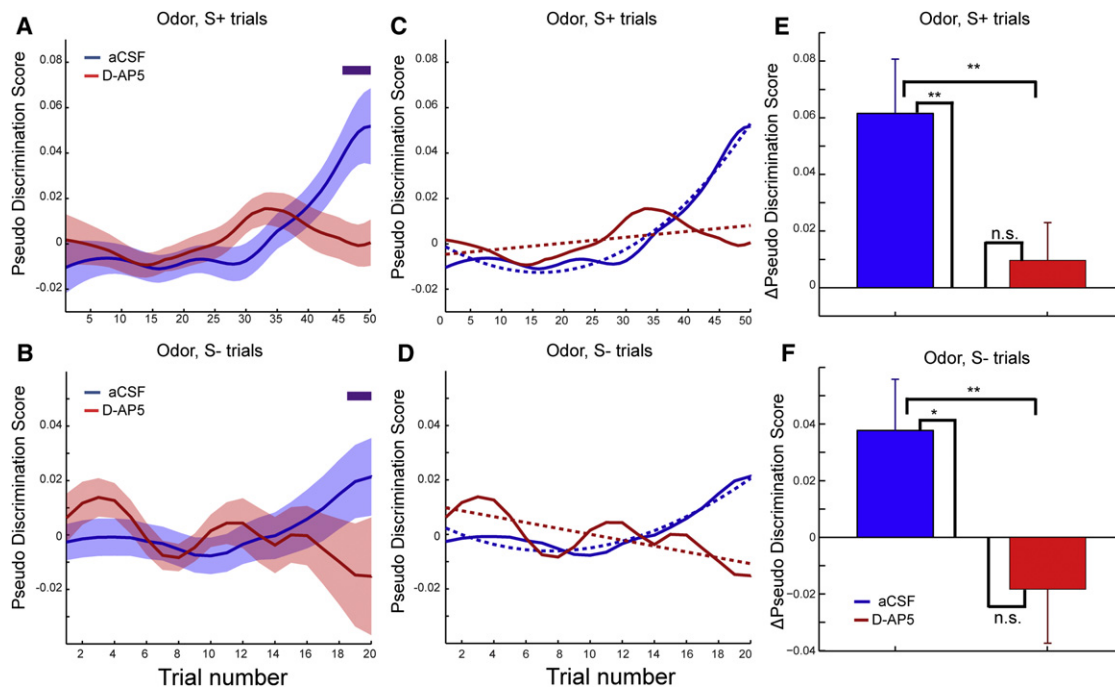
Figure 4. Evolution of Discrimination Scores over Acquisition Trials

(A and B) Bootstrapped mean of pseudodiscrimination scores for the acquisition odor phase against S+ (A) and S− (B) trial number. Positive pseudodiscrimination scores indicate that a trial contributed positively to overall ROC area. Shading indicates SD of bootstrap distribution. Horizontal purple lines indicate significant differences between group means (p < 0.05, Bonferroni corrected, bootstrap test).

(C) Best nonlinear fit (dashed lines) to the S+ group data (solid lines, as in A).

(D) as in (C), but now showing fits to the S− group data of (B).

(E) Bootstrapped mean difference in pseudodiscrimination scores between the first and the last trial of the acquisition phase (±SD across bootstraps). *, **p < 0.05, p < 0.01; bootstrap test.

(F) as in (E), but now for the S− odor period.

This difference may stem, first, from differential effects of systemic versus local OFC applications. Systemic injections may affect various stages of processing afferent to the OFC, e.g., in the mediodorsal thalamus, piriform cortex and basolateral amygdala. Second, in contrast to D-AP5, MK-801 acts as a dissociative anesthetic and impairs normal neural functioning, sometimes even causing cell damage and neuronal swelling (Olney et al., 1989). Whereas previous studies reported behavioral stereotypy induced by MK-801, we showed that behavioral patterns were not affected by local D-AP5 in the acquisition phase.

When considering a simplified circuit diagram of OFC pyramidal cells and interneurons (Figure 7), we may tentatively explain the trend toward lower baseline firing rates of putative pyramidal cells under D-AP5 by a reduction in recurrent OFC network activity due to low afferent stimulation in the absence of task-oriented behavior. When the animals were engaged in the task, no significant differences in absolute firing rates between pharmacological conditions were detected. These findings do not support a general pyramidal neuron "hyperexcitability" via a local reduction of NMDAR-mediated GABAergic inhibition (Homayoun and Moghaddam, 2007, 2008; Lisman et al., 2008), in line with a recent slice study indicating only a minor role for NMDARs in fast-spiking interneuron activity (Rotaru et al., 2011).

These findings are relevant for evaluating current hypotheses on schizophrenia. An involvement of NMDARs in schizophrenia is suggested by pharmacological studies of human volunteers subjected to non-specific NMDAR antagonists, such as ketamine, and recent postmortem studies on schizophrenic patients (Gilmour et al., 2012; Krystal et al., 2003; Lahti et al., 2001; Malhotra et al., 1997). The NMDAR hypofunction theory proposes that schizophrenia is associated with a reduction of NMDAR-mediated currents at pyramidal-interneuron synapses, resulting in low activity of interneurons and disinhibition of pyramidal neurons (Homayoun and Moghaddam, 2007; Lewis and Moghaddam, 2006; Lisman et al., 2008; Olney et al., 1999). Our data indicate that NMDAR blockade-induced hyperactivity in OFC does not arise strictly from local mechanisms, because a blockade did not significantly affect absolute firing rates of putative pyramidal neurons. Such hyperactivity likely arises from global interactions between OFC and other areas. Our data further suggest that the reduction in neuronal cue-outcome selectivity and plasticity could contribute to impairments in OFC-dependent sensory gating and cognitive function as reported in schizophrenic patients (Krystal et al., 2003; Lisman et al., 2008). Finally, consistent with theories regarding schizophrenia as a disorder of interareal connectivity (Lynall et al., 2010; Stephan et al., 2009), our data show that local NMDA
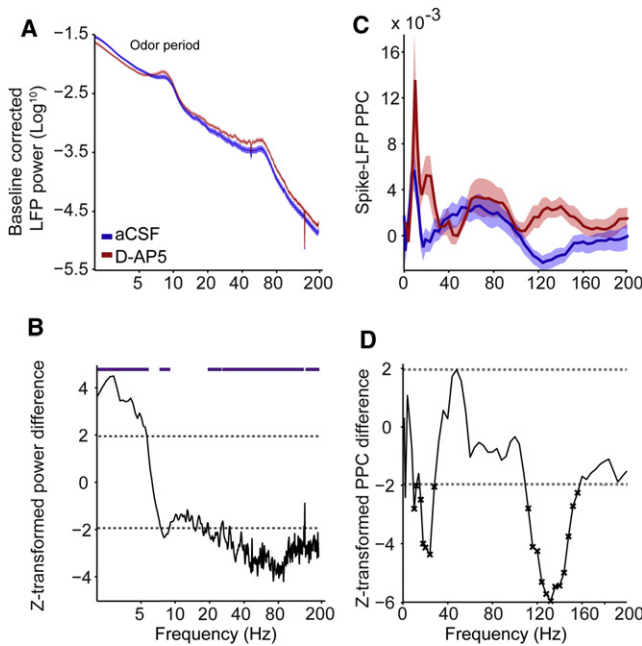
Figure 5. Effect of D-AP5 on Rhythmic Synchronization
(A) Average LFP power spectrum as a function of frequency. LFP power was normalized by dividing by the total LFP power across all analyzed frequencies. Shading indicates standard error of the mean. Spikes at 50 and 150 Hz were due to removing spectrally confined line noise.
(B) Z-transformed difference in relative LFP power spectrum as a function of frequency. Horizontal dashed lines: |1.96| SD thresholds; purple bars: p < 0.05, multiple comparison corrected (MCC) permutation test on T statistic.
(C) Spike-LFP PPC as a function of frequency. Shading indicates SEM.
(D) Z scored difference in PPC values between drug conditions, as a function of frequency. Crosses indicate significance at p < 0.05 (MCC permutation test on T statistics).
See also Figure S5.

hypofunction causes marked changes in spike-field phase-synchronization, which may result in global dysconnectivity between brain areas (Uhlhaas et al., 2008).

Orbitofrontal NMDA Receptors in Discriminating Stimulus-Outcome Patterns

In line with Schoenbaum et al. (1998, 1999), who demonstrated firing-rate selectivity in OFC for stimuli predictive of positive versus negative outcome, we found that during acquisition the electrophysiological S+/S− discrimination scores were significant during the entire task sequence from odor sampling to outcome delivery, both under drug and control conditions (Figure 3). D-AP5 diminished the discriminatory power of single units only during odor sampling. Under aCSF perfusion, the discrimination score during odor sampling increased over trials, due to adaptive changes in spike patterns across both S+ and S− trials (Figure 4). NMDAR blockade hampered the trial-dependent plasticity of discrimination scores across learning during the odor phase. The reduction in discrimination scores by NMDAR blockade cannot be attributed to a difference in absolute firing rates, because these did not differ significantly between pharmacological conditions for any behavioral period (Table 1). Upon

reversal, under D-AP5 perfusion, units lost their prereversal selectivity during cue sampling, while this selectivity was maintained for control units (Figure S3 and S4). Maintenance of neuronal cue selectivity has been linked to faster reversal learning (Schoenbaum et al., 2007; Stalnaker et al., 2006). Here, we show that this maintenance of neuronal cue selectivity is NMDAR-dependent. Altogether, these results support the conclusion that NMDAR blockade renders firing patterns of OFC units less robust in their discriminatory capacity during task acquisition and reversal, which may compromise the efficiency of OFC signaling during learning.

During acquisition, the discriminatory power of OFC neurons was strongly affected only in the odor period (Figure 3A). At first sight, these findings contrast with the reproducibly reported coding of outcome expectancy parameters by OFC neurons during post-decisional anticipation and processing of outcomes (O'Neill and Schultz, 2010; Schoenbaum et al., 1998, 1999; van Duuren et al., 2008). Because the present study combined recording with local intervention, it presents a strong case for an NMDAR-dependent mechanism in OFC for pre-decisional processing of stimulus information, coupled to the retrieval of odor-associated values predicting future outcome. Do NMDARs primarily support learning-related synaptic plasticity in OFC or are they of foremost importance in acute information processing due to their slow-EPSP contributions? We found that the firing discrimination score increased significantly with learning during S+ and S− odor sampling in control sessions (Figures 4A and 4B). On both S+ and S− trials, electrophysiological discrimination scores diverged between control and drug sessions with progressive learning, supporting the idea that learning-related plasticity of OFC firing patterns is reduced or lost with D-AP5 perfusion. Because the difference in discrimination scores between control and NMDAR blockade increased as learning progressed, the results suggest that OFC NMDARs are important for expressing long-term plasticity as underlying stimulus-outcome associative learning. Although our results do not prove that NMDA receptors mediate synaptic modifications within the OFC itself (because in theory they could also relay information acquired in afferent regions such as BLA; Groenewegen and Uylings, 2000; Mulder et al., 2003; Schoenbaum et al., 2003b), there are several indications that a mere relaying role can be considered unlikely. First, the NMDAR-mediated component of synaptic potentials in PFC is especially strong for recurrent, intracortical connections, not for excitatory inputs from afferent regions (Rotaru et al., 2011). Second, D-AP5 primarily affected OFC encoding during the cue period and much less so during the later trial periods of movement, waiting, and outcome. A crucial difference between the predecisional cue period and the postdecisional phases is that encoding of future outcome in these later periods does not necessarily depend on novel learning in the session under study, because it can rely on action patterns, cage- and fluid well-related cues that have already been associated with the outcome in previous learning sessions. If OFC NMDARs would merely relay previously acquired information from afferent regions, a stronger D-AP5 effect would have been expected also for these later trial periods. Nevertheless, this issue merits further investigation.
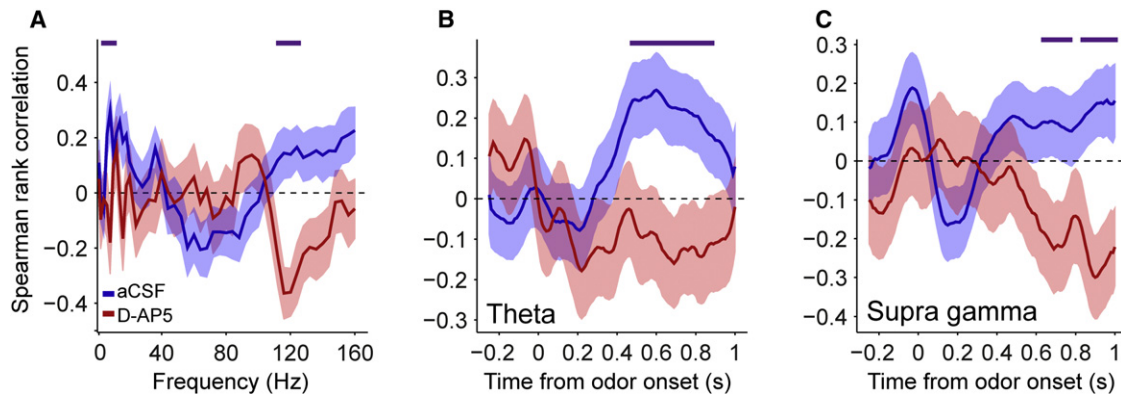
Figure 6. Relationship between Phase-Locking and Discrimination Scores

(A) Spearman rank correlations between spike-LFP phase consistency (PPC) and $D_{corrected}$ (shuffle-corrected ROC area) values during odor sampling period as a function of frequency for cells recorded under control (blue) and drug (red) conditions. Horizontal purple lines indicate significance at $p < 0.05$ (permutation-based multiple comparison correction).

(B) Spearman rank correlation between spike-LFP theta PPC (8–10 Hz, over entire odor sampling period) and time-resolved $D_{corrected}$ values relative to odor onset. Plot conventions as in (A).

(C) Same as (B), but now for spike-LFP supra-gamma PPC (115–130 Hz).

Regardless of the precise locus of plasticity, the question arises how NMDARs may support computational operations underlying decision making involving OFC. In addition to the implication of OFC NMDARs in decision making under reversal conditions (Bohn et al., 2003b), NMDARs in rat medial PFC affect appetitive instrumental learning (Baldwin et al., 2000). During odor discrimination learning, olfactory inputs need to be discriminated and should be associated with outcome value as signaled later in the trial. After initial learning, cue value must be associatively recalled and coupled to an appropriate behavioral decision. Before the decision is executed, however, cue and value information may need to be retained in working memory. While NMDARs could in principle contribute to all of these operations, a few possibilities stand out.

Pattern discrimination, perceptual decision-making and maintenance in working memory have been proposed to be mediated by recurrent neural networks (Figure 7, Lisman et al., 1998; Wang, 1999, 2002; Wong and Wang, 2006). In models of such networks, NMDARs on synapses between pyramidal cells contribute to reverberating, sustained activity capable of slow integration of sensory evidence over time. Recent studies showed that NMDARs at pyramidal-pyramidal synapses in the deep layers of rat prefrontal cortex mediate sustained depolarization, that sustained synaptic activity recorded in vivo from prelimbic cortex of anesthetized rats depended on NMDAR activity and that performance of a delayed-nonmatching to sample task was impaired by NMDAR antagonists in dorsal hippocampus (McHugh et al., 2008; Seamans et al., 2003; Wang et al., 2008). Although such discriminatory and temporally integrating mechanisms are predicted to operate during both early and late learning, the use and loading of recurrent network capacities may well change as learning progresses. In addition, OFC NMDARs may function in the actual updating of synaptic matrices encoding cue-outcome associations when reward contingencies are changing (Figure S1; cf. Bohn et al., 2003b).

Effect of NMDA Receptor Blockade on Rhythmic Synchronization

Rhythmic synchronization, i.e., coupling of oscillatory activity across neurons and populations, has been hypothesized to play a role in the temporal coordination of neuronal activity between separate brain areas (Battaglia et al., 2011; Fries, 2009). Previous studies showed increments in gamma-band coherence in the hippocampus and frontal areas of awake rodents after peripheral application of non-competitive NMDAR antagonists (Ma and Leung, 2007; Pinault, 2008). Using a competitive NMDAR blocker, we did not observe a significant difference in gamma-band spike-LFP phase-locking between control and drug sessions, and found that NMDAR blockade did not abolish changes in LFP gamma power over trials (Figure 5 and S5). Consistent with this discrepancy, an in vitro slice study showed that NMDAR blocking effects on gamma-band oscillations are highly dependent on the brain region under scrutiny and the mechanisms underlying gamma rhythmogenesis (Roopun et al., 2008). Slice studies further showed that NMDAR blockade increased the power of beta-band LFP oscillations in some areas (e.g., prelimbic and entorhinal cortex), but not in others (Middleton et al., 2008; Roopun et al., 2008). Thus, the emergence of a 20–25 Hz rhythm under a competitive NMDAR antagonist in behaving rats (Figure 5C) may likewise be regionally specific. The occurrence of phase locking to high-frequency (supra-gamma) oscillations with NMDAR blockade is consistent with a similar, ketamine-induced increase observed in high-frequency oscillations in the striatum of awake rats (Hunt et al., 2011).

Several recent studies indicated that firing-rate selectivity can be predicted from a neuron's pattern of synchronization to the LFP (Battaglia et al., 2011; Dean et al., 2012; Womelsdorf et al., 2012), suggesting that shared frequency and phase-of-firing preferences are a mechanism of neuronal assembly formation (Buzsáki, 2010; Fries, 2005; Singer, 1999). Here, we made
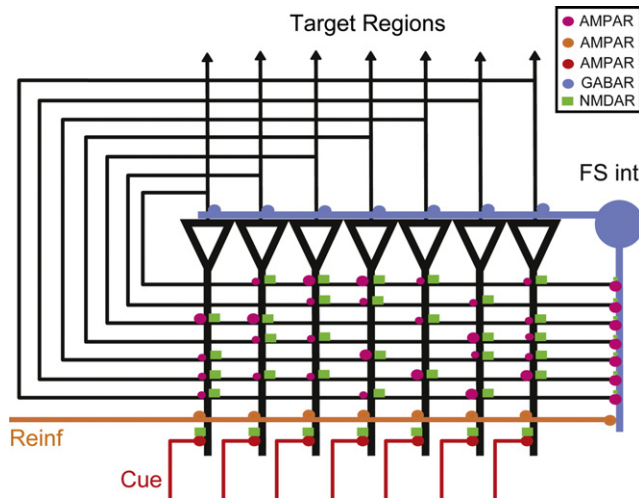
Figure 7. Simplified Circuit Diagram of OFC Network

Reduced circuit diagram of a local OFC network, showing cue- and reward-related afferent input (red/orange excitatory inputs) on pyramidal cells (black) and fast-spiking (FS) interneuron (blue; non-fast-spiking interneurons left out for simplicity). Pyramidal cells project axons that synapse both on cells in target regions and make local recurrent connections to other pyramidal cells and fast-spiking interneurons. Fast-spiking interneurons make inhibitory peri-isomatic synapses on pyramidal neurons using γ-aminobutyric acid receptors (GABAR, blue). Recurrent pyramidal-pyramidal synapses and pyramidal-interneuron synapses express both AMPA receptors (AMPAR, magenta) and NMDA receptors (NMDAR, green). The relative contribution of NMDAR-mediated excitatory input in recurrent pyramidal-pyramidal synapses is greater than in pyramidal-interneuron synapses. No NMDARs are included in the axons conveying reinforcement (Reinf; outcome-related) signals to the pyramidal cells, as modeling studies have indicated that such receptors may not be necessary for reinforcement learning.

a similar observation for the OFC: Neuronal firing rates were particularly selective to S+/S− conditions when their spiking activity was synchronized to the LFP theta rhythm (Figure 6). NMDAR blockade abolished this relationship (Figure 6) and reduced theta power over trials (Figure S5). In addition, it caused firing rates to become less odor/outcome-selective when spikes were synchronized to supra-gamma frequencies. Together, these findings suggest a role for OFC NMDARs not only in firing rate odor selectivity but also in rhythmic synchronization as a mechanism to support this selectivity.

EXPERIMENTAL PROCEDURES

Behavioral Task

The general behavioral methods of this experiment have been reported elsewhere (van Wingerden et al., 2010a, 2010b) and are reported in full in the Supplemental Experimental Procedures online. All experiments were conducted according to the National Guidelines on Animal Experiments and with approval of the Animal Experimentation Committee of the University of Amsterdam. Briefly, four male adult rats were trained on a two-odor go/no-go discrimination task (Figures 2A and 2B). Each session, two novel odors were presented to the rat in blocks of 5 + 5 pseudorandomly ordered trials with positive (S+) and negative (S−) outcome-predicting stimuli. Positive and negative outcomes were sucrose and quinine solutions, respectively. The behavioral sequence consisted of an ITI, onset of a light cuing trial onset, odor sampling period (>750 ms), go/no-go movement period, waiting period (with nose above fluid well, ≥1,000 ms) and outcome delivery. In the majority

of sessions (n = 15 out of 20), the acquisition period was immediately followed by a reversal period when a behavioral learning criterion was reached.

Recording Equipment

In order to combine simultaneous extracellular recording and local pharmacological manipulation, we adapted a microdrive to additionally hold a replaceable microdialysis probe (cf. van Duuren et al., 2007b). Spike and LFP recordings were made mainly from area VO/LO, with some spread in AI and DLO (Figure 1A).

Drug Perfusions

In drug sessions, a 0.5 mM D-AP5 solution dissolved in aCSF (artificial cerebrospinal fluid) was perfused at a speed of 4.0 μl/min through a probe membrane spanning 2 mm in the dorsoventral axis. Probe function was validated with perfusion of a 2% lidocaine solution, known to reversibly inhibit spiking of neurons recorded on nearby tetrodes (van Duuren et al., 2007b). Only units that responded to the wash-in and wash-out of the lidocaine solution were included for further analysis (281 out of 623 units).

Quantification of D-AP5 Concentration in OFC Tissue

Control experiments were performed on an additional seven rats, in which we applied radiolabeled D-[^{3}H]AP-5 in aCSF using the same device. Rats were sacrificed after either a 30 min or 2 hr perfusion period, and we inferred the spatial spread of D-AP5 from the activity profiles obtained at these time points (Figures 1B and 1C and Supplemental Experimental Procedures). We estimated effective D-AP5 concentrations in OFC tissue to be in the range of 5–10 μM. This range of drug concentrations is known from slice studies to have major blocking effects at NMDARs and to affect synaptic plasticity (Colino and Malenka, 1993; Cummings et al., 1996; Davies et al., 1981; Herron et al., 1986).

Analysis of Spike Data

Spikes were sorted into single unit data with automated algorithms (KlustaKwik and MClust 3.5) and manual refinement. We classified cells as responsive to the odor, movement, waiting or outcome period (as described in van Wingerden et al., 2010a, 2010b).

ROC Analysis

To quantify the ability of firing patterns to discriminate between the S+ and S− conditions, we performed an ROC analysis (cf. Green and Swets, 1966; Histed et al., 2009) on single-unit spike patterns, correcting for positive sampling bias through shuffle-correction (see Supplemental Experimental Procedures). Single trial contributions (pseudo-discrimination [PD] scores) to discriminatory power were calculated using a leave-one-out procedure. Learning-related correlations between PD values and trial number were assessed using a linear and a nonlinear regression of the type $y = a + bx + e^{cx}$ (Figures 4C and 4D) where x is trial number and y the average pseudodiscrimination score.

When reporting group data, we used the following "stratified bootstrap" procedure to remove the potential influence of systematic variance due to intersubject variability: on each bootstrap repetition, we randomly drew equal numbers (n = 50, with replacement) of units from the total pool of analyzed cells per rat for the drug and control condition. Group data are reported as means of such bootstrap populations ± SD of the bootstrap, which is a conventional estimate of the standard error of the original data (Chernick, 2008). To assess statistical differences, we compared the difference in bootstrapped means, divided by the average standard deviation of the bootstrap populations, to the normal distribution. We refer to this procedure as the "bootstrap test."

Analysis of Rhythmic Synchronization

Relative power spectra for the odor period were constructed by normalizing the raw power per frequency to the total power in the [2, 200] Hz interval (Figures 5A and 5B). Spike-LFP phase-locking was computed using the pairwise phase consistency method (see Supplemental Experimental Procedures; Vinck et al., 2012). As above, group averages were constructed using the stratified bootstrap procedure, and their significance was assessed by comparing the T-statistic of the bootstrap distribution to the normal distribution.

REFERENCES

Baldwin, A.E., Holahan, M.R., Sadeghian, K., and Kelley, A.E. (2000). N-methyl-D-aspartate receptor-dependent plasticity within a distributed corti-costriatal network mediates appetitive instrumental learning. Behav. Neurosci. *114*, 84–98.

Battaglia, F.P., Benchenane, K., Sirota, A., Pennartz, C.M., and Wiener, S.I. (2011). The hippocampus: hub of brain network communication for memory. Trends Cogn. Sci. *15*, 310–318.

Baxter, M.G., Parker, A., Lindner, C.C., Izquierdo, A.D., and Murray, E.A. (2000). Control of response selection by reinforcer value requires interaction of amygdala and orbital prefrontal cortex. J. Neurosci. *20*, 4311–4319.

Bi, G.Q., and Poo, M.M. (1998). Synaptic modifications in cultured hippocampal neurons: dependence on spike timing, synaptic strength, and postsynaptic cell type. J. Neurosci. *18*, 10464–10472.

Bohn, I., Giertler, C., and Hauber, W. (2003a). Orbital prefrontal cortex and guidance of instrumental behaviour in rats under reversal conditions. Behav. Brain Res. *143*, 49–56.

Bohn, I., Giertler, C., and Hauber, W. (2003b). NMDA receptors in the rat orbital prefrontal cortex are involved in guidance of instrumental behaviour under reversal conditions. Cereb. Cortex *13*, 968–976.

Bullmore, E.T., Suckling, J., Overmeyer, S., Rabe-Hesketh, S., Taylor, E., and Brammer, M.J. (1999). Global, voxel, and cluster tests, by theory and permutation, for a difference between two groups of structural MR images of the brain. IEEE Trans. Med. Imaging *18*, 32–42.

Buzsáki, G. (2002). Theta oscillations in the hippocampus. Neuron *33*, 325–340.

Buzsáki, G. (2010). Neural syntax: cell assemblies, synapsembles, and readers. Neuron *68*, 362–385.

Cassenaer, S., and Laurent, G. (2007). Hebbian STDP in mushroom bodies facilitates the synchronous flow of olfactory information in locusts. Nature *448*, 709–713.

Chernick, M.R. (2008). Bootstrap Methods: A Guide for Practitioners and Researchers, Second Edition (Hoboken, NJ: Wiley-Interscience).

Colino, A., and Malenka, R.C. (1993). Mechanisms underlying induction of long-term potentiation in rat medial and lateral perforant paths in vitro. J. Neurophysiol. *69*, 1150–1159.

Cummings, J.A., Mulkey, R.M., Nicoll, R.A., and Malenka, R.C. (1996). Ca2+ signaling requirements for long-term depression in the hippocampus. Neuron *16*, 825–833.

Davies, J., Francis, A.A., Jones, A.W., and Watkins, J.C. (1981). 2-Amino-5-phosphonovalerate (2APV), a potent and selective antagonist of amino acid-induced and synaptic excitation. Neurosci. Lett. *21*, 77–81.

De Bruin, J.P., Feenstra, M.G., Broersen, L.M., Van Leeuwen, M., Arens, C., De Vries, S., and Joosten, R.N. (2000). Role of the prefrontal cortex of the rat in learning and decision making: effects of transient inactivation. Prog. Brain Res. *126*, 103–113.

Dean, H.L., Hagan, M.A., and Pesaran, B. (2012). Only coherent spiking in posterior parietal cortex coordinates looking and reaching. Neuron *73*, 829–841.

Durstewitz, D., Seamans, J.K., and Sejnowski, T.J. (2000). Neurocomputational models of working memory. Nat. Neurosci. Suppl. *3*, 1184–1191.

Ekstrom, A.D., Meltzer, J., McNaughton, B.L., and Barnes, C.A. (2001). NMDA receptor antagonism blocks experience-dependent expansion of hippocampal "place fields". Neuron *31*, 631–638.

Fries, P. (2005). A mechanism for cognitive dynamics: neuronal communication through neuronal coherence. Trends Cogn. Sci. *9*, 474–480.

Fries, P. (2009). Neuronal gamma-band synchronization as a fundamental process in cortical computation. Annu. Rev. Neurosci. *32*, 209–224.

Gilmour, G., Dix, S., Fellini, L., Gastambide, F., Plath, N., Steckler, T., Talpos, J., and Tricklebank, M. (2012). NMDA receptors, cognition and schizophrenia—testing the validity of the NMDA receptor hypofunction hypothesis. Neuropharmacology *62*, 1401–1412.

Goosens, K.A., and Maren, S. (2004). NMDA receptors are essential for the acquisition, but not expression, of conditional fear and associative spike firing in the lateral amygdala. Eur. J. Neurosci. *20*, 537–548.

Green, D.M., and Swets, J.A. (1966). Signal Detection Theory and Psychophysics (New York: Wiley).

Groenewegen, H.J., and Uylings, H.B. (2000). The prefrontal cortex and the integration of sensory, limbic and autonomic information. Prog. Brain Res. *126*, 3–28.

Herron, C.E., Lester, R.A., Coan, E.J., and Collingridge, G.L. (1986). Frequency-dependent involvement of NMDA receptors in the hippocampus: a novel synaptic mechanism. Nature *322*, 265–268.

Hikosaka, K., and Watanabe, M. (2000). Delay activity of orbital and lateral prefrontal neurons of the monkey varying with different rewards. Cereb. Cortex *10*, 263–271.

Histed, M.H., Pasupathy, A., and Miller, E.K. (2009). Learning substrates in the primate prefrontal cortex and striatum: sustained activity related to successful actions. Neuron *63*, 244–253.

Homayoun, H., and Moghaddam, B. (2007). NMDA receptor hypofunction produces opposite effects on prefrontal cortex interneurons and pyramidal neurons. J. Neurosci. *27*, 11496–11500.

Homayoun, H., and Moghaddam, B. (2008). Orbitofrontal cortex neurons as a common target for classic and glutamatergic antipsychotic drugs. Proc. Natl. Acad. Sci. USA *105*, 18041–18046.

Hoover, W.B., and Vertes, R.P. (2011). Projections of the medial orbital and ventral orbital cortex in the rat. J. Comp. Neurol. *519*, 3766–3801.

Hunt, M.J., Falinska, M., Łeski, S., Wójcik, D.K., and Kasicki, S. (2011). Differential effects produced by ketamine on oscillatory activity recorded in the rat hippocampus, dorsal striatum and nucleus accumbens. J. Psychopharmacol. (Oxford) *25*, 808–821.

Jackson, M.E., Homayoun, H., and Moghaddam, B. (2004). NMDA receptor hypofunction produces concomitant firing rate potentiation and burst activity reduction in the prefrontal cortex. Proc. Natl. Acad. Sci. USA *101*, 8467–8472.

Jensen, O., and Lisman, J.E. (1996). Theta/gamma networks with slow NMDA channels learn sequences and encode episodic memory: role of NMDA channels in recall. Learn. Mem. *3*, 264–278.

Kentros, C., Hargreaves, E., Hawkins, R.D., Kandel, E.R., Shapiro, M., and Muller, R.V. (1998). Abolition of long-term stability of new hippocampal place cell maps by NMDA receptor blockade. Science *280*, 2121–2126.

Krystal, J.H., D'Souza, D.C., Mathalon, D., Perry, E., Belger, A., and Hoffman, R. (2003). NMDA receptor antagonist effects, cortical glutamatergic function, and schizophrenia: toward a paradigm shift in medication development. Psychopharmacology (Berl.) 169, 215–233.

Lahti, A.C., Weiler, M.A., Tamara Michaelidis, B.A., Parwani, A., and Tamminga, C.A. (2001). Effects of ketamine in normal and schizophrenic volunteers. Neuropsychopharmacology 25, 455–467.

Lee, H.K., Kameyama, K., Huganir, R.L., and Bear, M.F. (1998). NMDA induces long-term synaptic depression and dephosphorylation of the GluR1 subunit of AMPA receptors in hippocampus. Neuron 21, 1151–1162.

Lewis, D.A., and Moghaddam, B. (2006). Cognitive dysfunction in schizophrenia: convergence of gamma-aminobutyric acid and glutamate alterations. Arch. Neurol. 63, 1372–1376.

Li, X.F., Phillips, R., and LeDoux, J.E. (1995). NMDA and non-NMDA receptors contribute to synaptic transmission between the medial geniculate body and the lateral nucleus of the amygdala. Exp. Brain Res. 105, 87–100.

Lisman, J.E., Fellous, J.M., and Wang, X.J. (1998). A role for NMDA-receptor channels in working memory. Nat. Neurosci. 1, 273–275.

Lisman, J.E., Coyle, J.T., Green, R.W., Javitt, D.C., Benes, F.M., Heckers, S., and Grace, A.A. (2008). Circuit-based framework for understanding neurotransmitter and risk gene interactions in schizophrenia. Trends Neurosci. 31, 234–242.

Lynall, M.E., Bassett, D.S., Kerwin, R., McKenna, P.J., Kitzbichler, M., Muller, U., and Bullmore, E. (2010). Functional connectivity and brain networks in schizophrenia. J. Neurosci. 30, 9477–9487.

Ma, J., and Leung, L.S. (2007). The supramammillo-septal-hippocampal pathway mediates sensorimotor gating impairment and hyperlocomotion induced by MK-801 and ketamine in rats. Psychopharmacology (Berl.) 191, 961–974.

Malenka, R.C., and Nicoll, R.A. (1999). Long-term potentiation—a decade of progress? Science 285, 1870–1874.

Malhotra, A.K., Pinals, D.A., Adler, C.M., Elman, I., Clifton, A., Pickar, D., and Breier, A. (1997). Ketamine-induced exacerbation of psychotic symptoms and cognitive impairment in neuroleptic-free schizophrenics. Neuropsychopharmacology 17, 141–150.

Maris, E., Schoffelen, J.M., and Fries, P. (2007). Nonparametric statistical testing of coherence differences. J. Neurosci. Methods 163, 161–175.

McHugh, T.J., Jones, M.W., Quinn, J.J., Balthasar, N., Coppari, R., Elmquist, J.K., Lowell, B.B., Fanselow, M.S., Wilson, M.A., and Tonegawa, S. (2007). Dentate gyrus NMDA receptors mediate rapid pattern separation in the hippocampal network. Science 317, 94–99.

McHugh, S.B., Niewoehner, B., Rawlins, J.N., and Bannerman, D.M. (2008). Dorsal hippocampal N-methyl-D-aspartate receptors underlie spatial working memory performance during non-matching to place testing on the T-maze. Behav. Brain Res. 186, 41–47.

Middleton, S., Jalics, J., Kispersky, T., Lebeau, F.E., Roopun, A.K., Kopell, N.J., Whittington, M.A., and Cunningham, M.O. (2008). NMDA receptor-dependent switching between different gamma rhythm-generating microcircuits in entorhinal cortex. Proc. Natl. Acad. Sci. USA 105, 18572–18577.

Morris, R.G., Anderson, E., Lynch, G.S., and Baudry, M. (1986). Selective impairment of learning and blockade of long-term potentiation by an N-methyl-D-aspartate receptor antagonist, AP5. Nature 319, 774–776.

Mulder, A.B., Nordquist, R.E., Orgüt, O., and Pennartz, C.M. (2003). Learning-related changes in response patterns of prefrontal neurons during instrumental conditioning. Behav. Brain Res. 146, 77–88.

O'Neill, M., and Schultz, W. (2010). Coding of reward risk by orbitofrontal neurons is mostly distinct from coding of reward value. Neuron 68, 789–800.

Olney, J.W., Labruyere, J., and Price, M.T. (1989). Pathological changes induced in cerebrocortical neurons by phencyclidine and related drugs. Science 244, 1360–1362.

Olney, J.W., Newcomer, J.W., and Farber, N.B. (1999). NMDA receptor hypofunction model of schizophrenia. J. Psychiatr. Res. 33, 523–533.

Padoa-Schioppa, C., and Assad, J.A. (2006). Neurons in the orbitofrontal cortex encode economic value. Nature 441, 223–226.

Paxinos, G., and Watson, C. (2007). The Rat Brain in Stereotaxic Coordinates, Sixth Edition (Amsterdam: Academic Press/Elsevier).

Pennartz, C.M., van Wingerden, M., and Vinck, M. (2011a). Population coding and neural rhythmicity in the orbitofrontal cortex. Ann. N Y Acad. Sci. 1239, 149–161.

Pennartz, C.M.A., Ito, R., Verschure, P.F.M.J., Battaglia, F.P., and Robbins, T.W. (2011b). The hippocampal-striatal axis in learning, prediction and goal-directed behavior. Trends Neurosci. 34, 548–559.

Pinault, D. (2008). N-methyl d-aspartate receptor antagonists ketamine and MK-801 induce wake-related aberrant gamma oscillations in the rat neocortex. Biol. Psychiatry 63, 730–735.

Platt, M.L., and Glimcher, P.W. (1999). Neural correlates of decision variables in parietal cortex. Nature 400, 233–238.

Rolls, E.T., Hornak, J., Wade, D., and McGrath, J. (1994). Emotion-related learning in patients with social and emotional changes associated with frontal lobe damage. J. Neurol. Neurosurg. Psychiatry 57, 1518–1524.

Roopun, A.K., Cunningham, M.O., Racca, C., Alter, K., Traub, R.D., and Whittington, M.A. (2008). Region-specific changes in gamma and beta2 rhythms in NMDA receptor dysfunction models of schizophrenia. Schizophr. Bull. 34, 962–973.

Rotaru, D.C., Yoshino, H., Lewis, D.A., Ermentrout, G.B., and Gonzalez-Burgos, G. (2011). Glutamate receptor subtypes mediating synaptic activation of prefrontal cortex neurons: relevance for schizophrenia. J. Neurosci. 31, 142–156.

Schoenbaum, G., Chiba, A.A., and Gallagher, M. (1998). Orbitofrontal cortex and basolateral amygdala encode expected outcomes during learning. Nat. Neurosci. 1, 155–159.

Schoenbaum, G., Chiba, A.A., and Gallagher, M. (1999). Neural encoding in orbitofrontal cortex and basolateral amygdala during olfactory discrimination learning. J. Neurosci. 19, 1876–1884.

Schoenbaum, G.C.A., Nugent, S.L., Saddoris, M.P., and Setlow, B. (2002). Orbitofrontal lesions in rats impair reversal but not acquisition of go, no-go odor discriminations. Neuroreport 13, 885–890.

Schoenbaum, G., Setlow, B., Nugent, S.L., Saddoris, M.P., and Gallagher, M. (2003a). Lesions of orbitofrontal cortex and basolateral amygdala complex disrupt acquisition of odor-guided discriminations and reversals. Learn. Mem. 10, 129–140.

Schoenbaum, G., Setlow, B., Saddoris, M.P., and Gallagher, M. (2003b). Encoding predicted outcome and acquired value in orbitofrontal cortex during cue sampling depends upon input from basolateral amygdala. Neuron 39, 855–867.

Schoenbaum, G., Saddoris, M.P., and Stalnaker, T.A. (2007). Reconciling the roles of orbitofrontal cortex in reversal learning and the encoding of outcome expectancies. Ann. N Y Acad. Sci. 1121, 320–335.

Schoenbaum, G., Roesch, M.R., Stalnaker, T.A., and Takahashi, Y.K. (2009). A new perspective on the role of the orbitofrontal cortex in adaptive behaviour. Nat. Rev. Neurosci. 10, 885–892.

Seamans, J.K., Nogueira, L., and Lavin, A. (2003). Synaptic basis of persistent activity in prefrontal cortex in vivo and in organotypic cultures. Cereb. Cortex 13, 1242–1250.

Selig, D.K., Hjelmstad, G.O., Herron, C., Nicoll, R.A., and Malenka, R.C. (1995). Independent mechanisms for long-term depression of AMPA and NMDA responses. Neuron 15, 417–426.

Singer, W. (1999). Neuronal synchrony: a versatile code for the definition of relations? Neuron 24, 49–65, 111–125.

Stalnaker, T.A., Roesch, M.R., Franz, T.M., Burke, K.A., and Schoenbaum, G. (2006). Abnormal associative encoding in orbitofrontal neurons in cocaine-experienced rats during decision-making. Eur. J. Neurosci. 24, 2643–2653.

Stephan, K.E., Friston, K.J., and Frith, C.D. (2009). Dysconnection in schizophrenia: from abnormal synaptic plasticity to failures of self-monitoring. Schizophr. Bull. *35*, 509–527.

Sugrue, L.P., Corrado, G.S., and Newsome, W.T. (2005). Choosing the greater of two goods: neural currencies for valuation and decision making. Nat. Rev. Neurosci. *6*, 363–375.

Tremblay, L., and Schultz, W. (2000a). Reward-related neuronal activity during go-nogo task performance in primate orbitofrontal cortex. J. Neurophysiol. *83*, 1864–1876.

Tremblay, L., and Schultz, W. (2000b). Modifications of reward expectation-related neuronal activity during learning in primate orbitofrontal cortex. J. Neurophysiol. *83*, 1877–1885.

Uhlhaas, P.J., Haenschel, C., Nikolić, D., and Singer, W. (2008). The role of oscillations and synchrony in cortical networks and their putative relevance for the pathophysiology of schizophrenia. Schizophr. Bull. *34*, 927–943.

van Duuren, E., Escámez, F.A., Joosten, R.N., Visser, R., Mulder, A.B., and Pennartz, C.M. (2007a). Neural coding of reward magnitude in the orbitofrontal cortex of the rat during a five-odor olfactory discrimination task. Learn. Mem. *14*, 446–456.

van Duuren, E., van der Plasse, G., van der Blom, R., Joosten, R.N., Mulder, A.B., Pennartz, C.M., and Feenstra, M.G. (2007b). Pharmacological manipulation of neuronal ensemble activity by reverse microdialysis in freely moving rats: a comparative study of the effects of tetrodotoxin, lidocaine, and muscimol. J. Pharmacol. Exp. Ther. *323*, 61–69.

van Duuren, E., Lankelma, J., and Pennartz, C.M.A. (2008). Population coding of reward magnitude in the orbitofrontal cortex of the rat. J. Neurosci. *28*, 8590–8603.

van Wingerden, M., Vinck, M., Lankelma, J., and Pennartz, C.M. (2010a). Theta-band phase locking of orbitofrontal neurons during reward expectancy. J. Neurosci. *30*, 7078–7087.

van Wingerden, M., Vinck, M., Lankelma, J.V., and Pennartz, C.M. (2010b). Learning-associated gamma-band phase-locking of action-outcome selective neurons in orbitofrontal cortex. J. Neurosci. *30*, 10025–10038.

Vinck, M., van Wingerden, M., Womelsdorf, T., Fries, P., and Pennartz, C.M. (2010). The pairwise phase consistency: a bias-free measure of rhythmic neuronal synchronization. Neuroimage *51*, 112–122.

Vinck, M., Battaglia, F.P., Womelsdorf, T., and Pennartz, C. (2012). Improved measures of phase-coupling between spikes and the local field potential. J. Comput. Neurosci. *33*, 53–75.

Wallis, J.D., and Miller, E.K. (2003). Neuronal activity in primate dorsolateral and orbital prefrontal cortex during performance of a reward preference task. Eur. J. Neurosci. *18*, 2069–2081.

Walton, M.E., Behrens, T.E., Buckley, M.J., Rudebeck, P.H., and Rushworth, M.F. (2010). Separable learning systems in the macaque brain and the role of orbitofrontal cortex in contingent learning. Neuron *65*, 927–939.

Wang, X.J. (1999). Synaptic basis of cortical persistent activity: the importance of NMDA receptors to working memory. J. Neurosci. *19*, 9587–9603.

Wang, X.J. (2002). Probabilistic decision making by slow reverberation in cortical circuits. Neuron *36*, 955–968.

Wang, H., Stradtman, G.G., 3rd, Wang, X.J., and Gao, W.J. (2008). A specialized NMDA receptor function in layer 5 recurrent microcircuitry of the adult rat prefrontal cortex. Proc. Natl. Acad. Sci. USA *105*, 16791–16796.

Womelsdorf, T., Lima, B., Vinck, M., Oostenveld, R., Singer, W., Neuenschwander, S., and Fries, P. (2012). Orientation selectivity and noise correlation in awake monkey area V1 are modulated by the γ cycle. Proc. Natl. Acad. Sci. USA *109*, 4302–4307.

Wong, K.F., and Wang, X.J. (2006). A recurrent network mechanism of time integration in perceptual decisions. J. Neurosci. *26*, 1314–1328.